Thermal modeling of a secondary concentrator integrated with an open direct-absorption molten-salt volumetric receiver in a beam-down tower system

Citation: Lahlou, Radia, Peter Armstrong, Benjamin Grange, Saif Almheiri, Nicolas Calvet, Alexander Slocum, and Tariq Shamim. "Thermal Modeling of a Secondary Concentrator Integrated with an Open Direct-Absorption Molten-Salt Volumetric Receiver in a Beam-down Tower System" AIP Conference Proceedings 1734, AIP Publishing, 2016 . © 2016 Authors

As Published: http://dx.doi.org/10.1063/1.4949036

Publisher: AIP Publishing

Persistent URL: http://hdl.handle.net/1721.1/120000

Version: Final published version: final published article, as it appeared in a journal, conference proceedings, or other formally published context

Thermal Modeling of a Secondary Concentrator Integrated with an Open Direct-Absorption Molten-Salt Volumetric Receiver in a Beam-Down Tower System

Radia Lahlou[1, a)], Peter Armstrong[1], Benjamin Grange[1], Saif Almheiri[1], Nicolas Calvet[1], Alexander Slocum[2] and Tariq Shamim[1]

[1] *Institute Center for Energy (iEnergy), Department of Mechanical & Materials Engineering, Masdar Institute of Science & Technology, Masdar City, P.O. Box 54224, Abu Dhabi, United Arab Emirates.*
[2] *Department of Mechanical Engineering, Massachusetts Institute of Technology, 77 Massachusetts Ave, Cambridge, MA 02139, United States of America*

[a)] Corresponding author: rlahlou@masdar.ac.ae

Abstract. An upward-facing three-dimensional secondary concentrator, herein termed Final Optical Element (FOE), is designed to be used in a beam-down tower in combination with an open volumetric direct-absorption molten-salt receiver tank acting simultaneously as a thermal energy storage system. It allows reducing thermal losses from the open receiver by decreasing its aperture area while keeping minimal spillage losses. The FOE is exposed to high solar fluxes, a part of which is absorbed by its reflector material, leading to material degradation by overheating. Consequently, the FOE may require active cooling. A thermal model of the FOE under passive cooling mechanism is proposed as a first step to evaluate its sensitivity to some design parameters. Then, it will be used to evaluate the requirements for the active cooling system. The model provides insights on the FOE thermal behavior and highlights the effectiveness of a design modification on passive cooling enhancement. First prototype tests under reduced flux and with no active cooling will be used for model adjustment.

INTRODUCTION

Concentrated Solar Power on Demand (CSPonD) Demo Project

CSPonD Concept

The current work is part of the CSPonD (Concentrated Solar Power on Demand) Demo project[1] which aims at designing and testing a CSPonD prototype at the 100 kW_{th} Beam-Down Tower[2] at the Masdar Institute Solar Platform.

The CSPonD concept[3] consists of a single molten salt tank acting both as an open volumetric direct-absorption receiver and a thermal energy storage (TES) system. As shown in Fig.1 (a), concentrated solar flux from the beam-down tower enters the tank from an open aperture at the top and is directly absorbed in the volume of the semi-transparent nitrate molten salts (solar salt). An actuated loose-fitting insulated raft, called divider plate, is used to separate the hot and cold salt regions, enhancing the natural stratification effect. Thus, the single tank simultaneously acts as a volumetric receiver and TES. In charging/discharging mode, the vertical movement of the divider plate is actuated downwards/upwards respectively, allowing controlled salt transfer from one region to the other through the circumferential annular gap, in order to maintain constant temperatures of the hot and cold salt regions. The divider plate includes a mixing enhancement system in the hot region (not shown in Fig. 1) to ensure temperature homogeneity. Salts at 550 °C are extracted from the upper tank and injected back at the bottom at 280

SolarPACES 2015
AIP Conf. Proc. 1734, 020012-1–020012-9; doi: 10.1063/1.4949036
Published by AIP Publishing. 978-0-7354-1386-3/$30.00

°C after flowing through a heat exchanger. During the nominal 8-hour charging period, the system is designed to absorb 600 kWh, of which 200 kWh is delivered at a fixed rate of 25 kW and the remaining 400 kWh is stored.

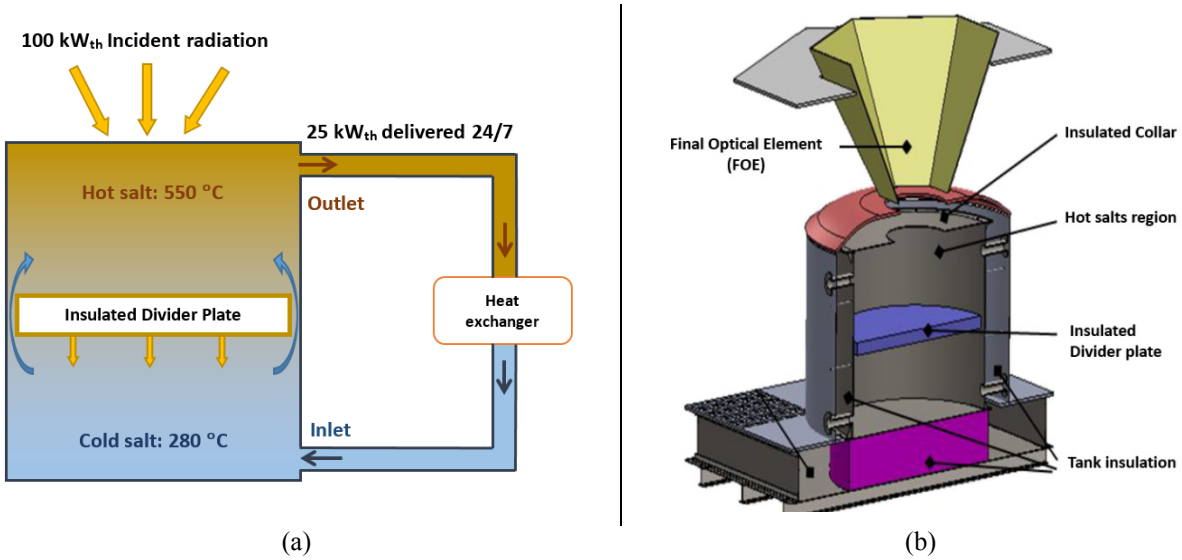

(a) (b)

FIGURE 1. CSPonD Demo concept; (a) schematic of operating principle -charging mode, (b) Cross section of the CSPonD system layout with integrated secondary concentrator (FOE), designed for the first prototype tests within the current demo project

The single-tank combined receiver and TES concept presents potential advantages through elimination of secondary hot and cold salt storage tanks and associated molten salt pumps as well as the inefficiencies of transferring heat to separate storage systems. Additionally, compared to conventional tubular surface absorption systems, the volumetric absorption within the salts overcomes limitations such as tubes thermal fatigue and rupture and frees the system from high pressure circulation pumps. The open-air design eliminates the use of quartz windows which are susceptible to various failure modes.

Final Optical Element (FOE)

In order to compensate for the beam-down system inherent magnification effect[4], an upward-facing 3D-secondary concentrator[*], designated in this paper by final optical element (FOE), is used at the aperture of the tank. Figure 1 (b) shows the layout of the first prototype system where a movable FOE is integrated with the open CSPonD tank, thus allowing for tank closure by an insulated lid whenever sufficient solar flux is not available.

The existing beam-down layout and central reflector canting yields a ~25° incident half-angle from the central reflectors edge rays- which allow for an additional theoretical concentration ratio up to ~ 5 by the use of a 3D-secondary concentrator[1]. The additional concentration introduced by the FOE allows reducing radiative and convective thermal losses from the open receiver by decreasing its aperture area while keeping minimal spillage losses. A conical-shaped FOE has been selected over a compound parabolic concentrator (CPC) shape. Ray-tracing optical simulations[1] revealed that a conical shape produces a more uniform flux distribution with better axial alignment of rays at its outlet. Moreover, the simulations showed that a "6-facet cone" shape (hexagonal cross section) provides comparable performance to the regular cone shape. Therefore, a faceted-cone has been selected for the current prototype due to ease of manufacturing.

Typical reflecting materials used in secondary concentrators are thin silvered glass or enhanced aluminum reflectors[5]. For the project's first prototype, polished aluminum was chosen as it was the cheapest and easiest option despite its relatively low specular reflectance. Use of enhanced aluminum or other better reflectors is envisaged for the next phase. Aluminum reflectors are preferred to glass mirrors as they offer better endurance to possible shocks induced by manipulation of the movable FOE.

Three dimensional secondary concentrators are exposed to high radiation fluxes, a part of which is absorbed by the reflecting material leading to elevated wall temperatures and most likely material degradation and thermal

[*] In the beam-down configuration, the final optical element acts as a secondary concentrator; the primary concentrator being the heliostat field. It is not to be confused with the central reflectors at the top of the tower which are sometimes called secondary reflectors –not concentrators-.

expansion. Reflectance loss from exposure to high temperatures[5] would lead to even higher absorbed flux.

Three dimensional secondary concentrators are typically water-cooled and kept at a temperature around 85 °C [5] to keep cooling water in liquid state and avoid possible degradation of the glue if applicable. However, for our open tank concept, water-cooling of FOE is not desirable in order to avoid any possible water intrusion in the molten salt tank, as contact of water and hot molten nitrate salts presents risks of explosive generation of steam[6]. The maximum acceptable temperature in our case depends on the reflecting material behavior with temperature –reflectance loss, thermal expansion, etc. - and will be defined once these characteristics are studied.

Scope of Work

A numerical model of the selected FOE thermal behavior without active cooling is developed and used to simulate operation under extreme conditions of solar irradiation and surrounding factors, namely incident flux of 115 kW and ambient temperature of 50 °C. Sensitivity studies are conducted to evaluate effects of some design parameters on the passive cooling behavior. Such model is employed, in a first stage, to analyze the temperature profile and critical regions in the FOE wall. At a later stage, the model will be modified to evaluate the effectiveness and limits of different cooling concepts. The present model allows as well for identification of suitable locations for temperature measurements for the first prototype testing. The model will be adjusted by using experimental results.

MODEL DESCRIPTION

Figure 2 (a) shows the heat transfer modes affecting the FOE temperature. Incident solar heat flux density is increasing from top to bottom of the FOE. The absorbed flux depends on local wall reflectance as well as local incident flux. Natural convection and radiation affecting the outer wall and inner wall are treated separately and referred to as *external* and *internal* respectively. External natural convection involves ambient air only, while internal convection is affected by the air temperature and movement in the inner domain where complex air flow patterns are present. This is due to the high temperature of tank walls and salt surface, up to 550 °C, and the geometry of the inner domain that is closed from the bottom and open to ambient from the top. Internal radiation lies in the exchange between the FOE inner surface, the outer surroundings and the tank. The radiative emission coming out of the tank, part of which is intercepted by the inner surface, comprises three parts: 1) volumetric emission within the salt that is transmitted through the salt, 2) emission from the divider plate stainless-steel top surface that is transmitted through the salt, 3) emission from the stainless-steel-tank side walls and the ceramic wall. Reflection of solar irradiation by salt surface or ceramic wall that may be intercepted by the FOE is neglected. Conduction within the FOE wall is also a distinct, albeit relatively minor heat transfer mode in the subsystem of interest.

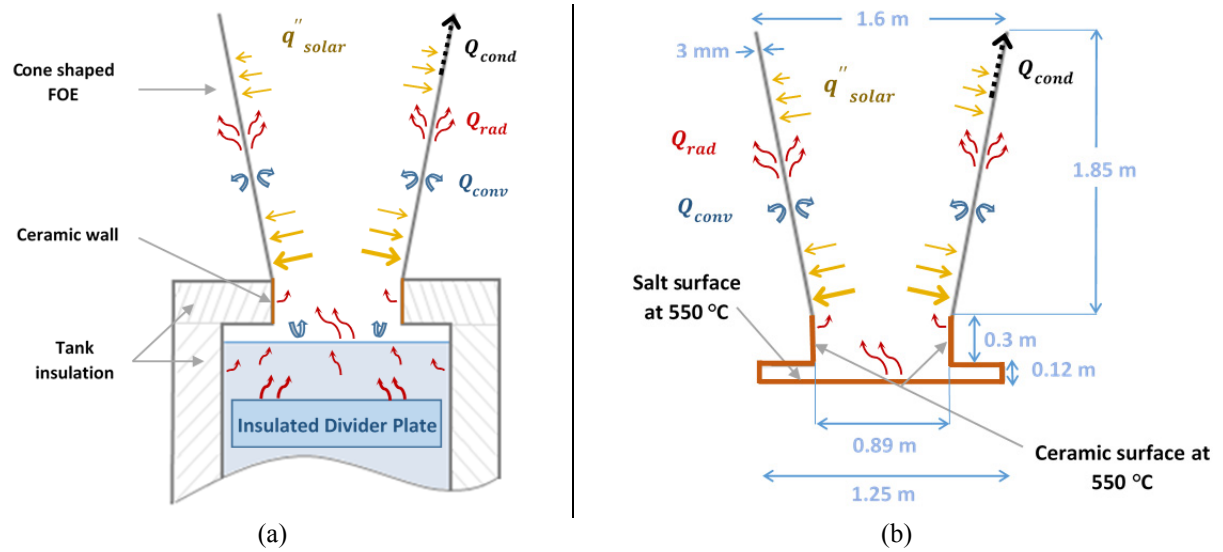

FIGURE 2. Schematic of heat transfer modes affecting the FOE temperature; (a) Full-modes schematic, (b) Simplified tank-radiation model developed in the current study using ANSYS Mechanical. q''_{solar} stands for the incident solar flux density and Q_{cond}, Q_{rad}, Q_{conv} for the conductive, radiative and convective heat fluxes.

The current study presents a simplified thermal model developed using the structural finite element analysis (FEA) tool ANSYS Mechanical which includes a thermal analysis component. It is based on input convection coefficients and built-in modeling of grey-diffuse surface-to-surface radiation through non-participating media. A schematic of the simplified geometry and heat transfer modes is presented in Fig. 2 (b). The FOE is represented by a regular cone instead of the faceted-cone used in the prototype in order to keep geometrical symmetry, and the tank is represented by a surface body symbolized by orange lines on the figure.

The present model was used to study the impact of the presence of an emitting body at the bottom under most extreme case by simulating the tank surface at a constant temperature, 550 °C, and setting the emissivity of the salt surface to 1. It showed a limited impact of the radiation from the tank, due to view factors and low emissivity -hence low absorptivity in infrared- of the aluminum material used as a reflector for the current FOE prototype. Therefore, accounting for the exact radiative emission out of the tank as presented in Fig.2 (a) is not necessary, especially given the desired level of accuracy.

The current model is used to evaluate the effect of different values of air temperature and convective coefficients in the inner domain by means of a sensitivity study. It does not capture the complex natural convection behavior in the inner domain described earlier, as the correct air temperature and convection coefficients cannot be estimated. The natural convection in the inner domain can only be modeled by computational fluid dynamics (CFD). However, turbulent natural convection in open domain is delicate to model and can be considered as a separate field of study.

The following assumptions, to be further detailed in the specifications section, are used in the current model:

- **General:** steady-state, most extreme conditions, ambient temperature 50 °C for convection and radiation.
- **Conduction:** constant conductivity with temperature as effect of temperature-dependent value is negligible.
- **Natural convection:** *External***:** using wall-temperature-dependent convective coefficients calculated from correlations for heated inclined plates; main assumption of the correlation is a constant wall temperature along the height. *Internal*: not included in the base case. Sensitivity study of effect of different values of convective coefficient and air temperature is performed.
- **Radiation:** All surfaces are assumed grey and diffuse as imposed by the software. Ambient air temperature is used for radiation with the surroundings which are assumed as a black-body. *External***:** radiation set as "to ambient", meaning to surroundings, using a defined surface emissivity and a view factor of 1; *Internal:* set as "surface-to-surface" radiation in an enclosure comprising the FOE inner wall and the tank inner surfaces and set as "open", meaning that it can radiate with ambient surroundings through the gaps. Tank inner surfaces are represented by ceramic and salt surfaces only, as the remaining surfaces are not being viewed by the cone, cf. Fig. 2 (b), and set to a constant temperature of 550 °C.
- **Absorbed heat flux density:** Incident flux is obtained from ray-tracing simulations of the whole optical system (beam-down optical system and FOE). Material is assumed of constant reflectance on all the surface and purely specular, i.e. hemispherical reflectance is equal to specular reflectance ρ_s, so that absorbed flux is (1- ρ_s) times incident flux. The software only supports constant flux density on a surface, thus the geometry is discretized vertically in 10 slices and a constant corresponding averaged flux density is defined on each slice.

First on-sun prototype tests are planned to start in the Fall of 2015. A polished-aluminum FOE integrated to a water-filled tank will be tested. Incident flux will be gradually increased by incremental deployment of heliostats while FOE temperatures are monitored. Once the experimental protocol is defined, current model inputs (shape, incident flux, ρ_s …) will be set accordingly for comparison with experimental results and model adjustment.

Specifications

All cases are run in steady-state as a case run in transient mode showed that the steady-state is almost reached within 20 min starting from 50 °C as a wall temperature. The simulated incident solar flux is taken at solar noon on June 21st (zenith angle~1°) where the total incident flux on FOE is 115 kW with DNI = 796 W/m^2. Flux density values obtained from ray-tracing optical model are first averaged over horizontal slices of 0.014 m height. As both incident and absorbed flux are dependent on FOE's reflectance which depends on the choice and state of reflecting material, two extreme reflectance values are simulated to represent the case of a "poor" reflector with ρ_s = 0.6 and a "fair" reflector with ρ_s = 0.8. Figure 3 (a) and (b) show the absorbed flux density distribution along the FOE height for 0.8 and 0.6 reflectance respectively. Red diamonds show the averaged values over slices of 0.185 m used as

inputs in the current model. It can be noticed that the flux density is significantly higher on the FOE bottom part which leads to issues presented in the results section.

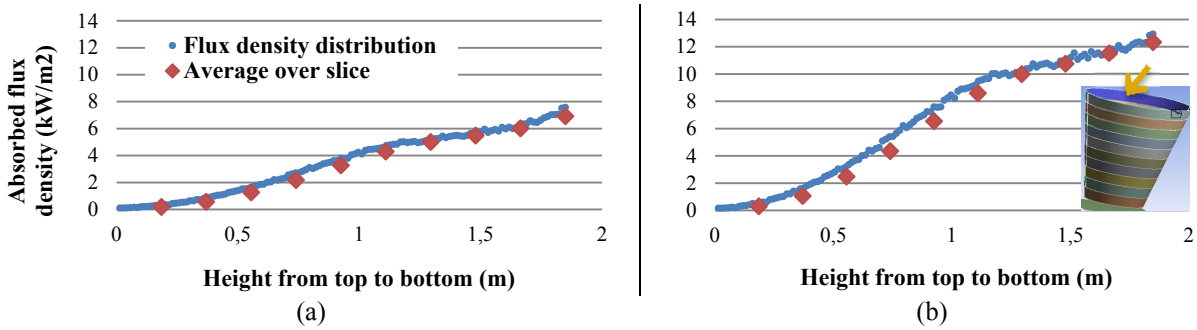

FIGURE 3. Absorbed flux distribution on FOE inner wall from ray-tracing simulation at solar noon, June 21st, integrated over horizontal slices of 0.014m height (blue) or 0.185 m (red); (a) Specular reflectance $\rho_s = 0.8$, (b) Specular reflectance $\rho_s = 0.6$

Temperature-dependent convective coefficients for the outer wall have been calculated using Churchill and Chu[7] correlation for turbulent natural convection on heated vertical plates. According to Rich[8], this correlation applies to the bottom surface of heated inclined plates by correcting the gravity term in the Grashof number with the cosine of the inclination angle. The correlation is also valid for vertical cylinders if the diameter to length ratio satisfies the Sparrow[9] condition. This condition applies in our case by approximating the cone as a cylinder of diameter equal to the cone bottom diameter. The only assumption that could be a source of considerable error is that correlations assume a constant wall temperature along the height, which doesn't apply in the present case. Calculated values of convective coefficient vary from 2.3 W/m^2/K for a wall temperature of 55 °C to 6.9 W/m^2/K for 600 °C.

For 'surface-to-surface' radiation in an enclosure, ANSYS Mechanical performs a radiosity calculation based on view factors calculated using the Hemicube method. For "open" surface-to-surface radiation where the surfaces of the enclosure can radiate to the ambient surroundings through the gaps, the temperature of the surroundings is set to 50 °C. "Perfect" enclosure can be defined as well for surface-to-surface radiation to artificially exclude the radiation with surroundings through the gaps.

The base case has the following specifications which represent the case of an aluminum reflector with a fair reflectance. The other cases presented in the results section have a variation in one or more parameters from the base case. Reflectance is taken as $\rho_s = 0.8$. Conductivity is set as $k = 237.5$ W/m/K and the cone thickness is 3 mm. Convection at the outer wall is specified by the above-mentioned calculated temperature-dependent convective coefficients and ambient air temperature is 50 °C. No internal convection is included. Emissivity of the FOE is $\varepsilon = 0.1$ for both inner and outer walls. Internal radiation is set as an "open" surface-to-surface radiation within an enclosure containing the inner FOE wall and the ceramic and salt surfaces representing the tank. Both surfaces are set to 550 °C to represent a worst possible case, ceramic emissivity is known and is set to $\varepsilon = 0.3$ and salt surface emissivity is taken as $\varepsilon = 1$ to represent an extreme case. All cases use 9700 elements for the FOE, defined after a mesh sensitivity study.

RESULTS

Figures 4 (a) and (b) show the temperature distribution along the FOE wall for reflectance values of $\rho_s = 0.8$ and $\rho_s = 0.6$, respectively. All other parameters are as described for the base case. Note that these results do not account for the internal convection, which will be evaluated by a sensitivity study in the following paragraphs. Also, the included radiation from the tank is not representing reality as it depicts a maximum possible emission out of the tank.

As expected, temperatures are significantly higher for the lower reflectance case due to increased absorbed flux. It shows that a low reflectance value not only leads to optical losses, but also increases considerably the cooling requirements of the FOE. Reflector material choice has therefore a central role in the FOE thermal behavior.

The critical zone of the FOE, where the temperature is the highest, is the bottom. The incident flux is much higher at the bottom than at the top, and the temperature difference between the upper and bottom parts is quite significant. The bottom has also a smaller heat transfer surface area compared to the upper part, which reduces the outer heat dissipation to ambient. As for its inner surface, it is in proximity to the tank hot region while the upper

inner surface may have further natural convection cooling effect due to its proximity to ambient air. In the following analysis, focus will be on reduction of the maximum temperature which corresponds to the FOE bottom. In addition to sensitivity analyses, effects of passive cooling enhancements are presented. Description and results of the analyzed cases are summarized in Table 1.

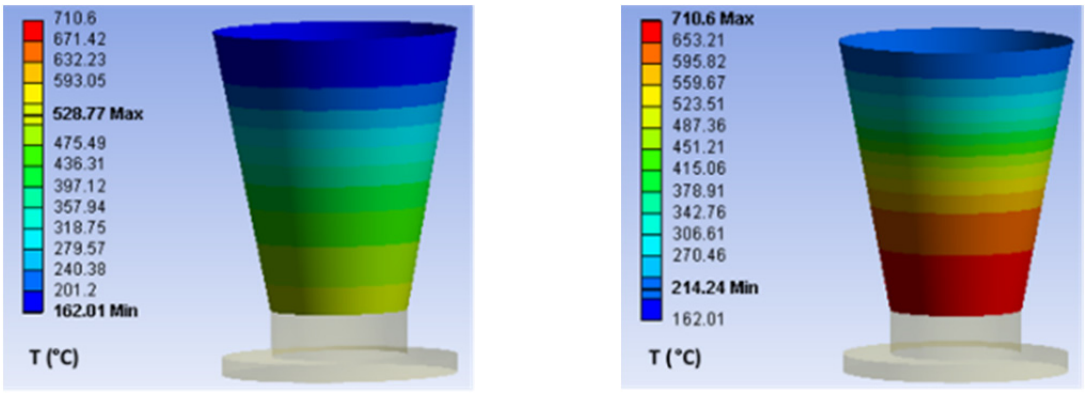

(a) (b)

FIGURE 4. Temperature distribution along the FOE a) Base case: specular reflectance $\rho_s = 0.8$; (b) case 1: $\rho_s = 0.6$

Temperature Homogenization

Test cases were run to evaluate the temperature homogenization effect between bottom and upper cone parts by means of conduction and internal cone-to-cone radiation. To assess the impact of aluminum's high conductivity on reducing the temperature difference between the top and the bottom, case 2 shows results with a much lower conductivity- simulating the use of glass reflectors-. Comparing the base case with these temperature values, it appears that a high conductivity has indeed an effect in transferring heat from the bottom to the top, thus reducing the maximum temperature (bottom) and increasing the minimum temperature (top). The temperature difference is reduced by ~ 95 °C in the case of the high conductivity value of aluminum. However, this effect is not sufficient to effectively dissipate the heat to the top and hence reduce the high bottom temperature. This is due to the cone's very low thickness, 3 mm, compared to its height, 1.85 m. Case 3 shows that a slightly higher thickness, 5 mm, yields to a slightly lower temperature difference than the base case but its effect is not significant enough to justify increasing the wall thickness.

As for internal cone-to-cone radiation effect on reducing the thermal stratification, it can be evaluated from cases 4, 5 and 6. In cases 5 and 6, cone-to-cone radiation is simulated by suppressing the tank surface and specifying a "perfect" enclosure surface-to-surface radiation on the cone inner wall to exclude radiation with ambient surroundings. As compared to case 4 where no internal radiation is accounted for, case 5 shows a reduction in the temperature difference by ~ 110 °C through introducing a cone-to-cone radiation. In a hypothetical case of internal emissivity of 1-which could not be achieved with aluminum reflectors- as shown in case 6, the temperature difference is reduced by 270 °C. Cone-to-cone radiation has therefore a bigger effect in homogenization than axial conduction, but both effects combined still yield important temperature difference between top and bottom as exhibited by the base case.

Effect of Radiation

The internal radiation applied in the base case includes three effects: temperature homogenization due to cone-to-cone radiation, radiation of cone with ambient, and effect of radiation exchange with the tank. The three effects have been studied separately and the first one has been presented in the previous paragraph. Radiation to ambient from inner wall can be evaluated by comparing cases 5 and 9. In case 9, the tank is suppressed and "open" enclosure surface-to-surface radiation is applied on the inner wall, allowing for both cone-to-cone and cone-to-ambient radiation. Compared to case 5 which accounts for cone-to-cone radiation only, the minimum temperature is reduced by ~ 80 °C and the maximum temperature by ~ 40 °C only. The radiation from the inner wall to ambient has therefore a lower tempering effect on the bottom part than on the top part of the cone.

Effect of radiation between cone and tank is assessed by cases 5, 7 and 8. Comparing cases 5 and 7, it appears that the presence of the tank at 550 °C increases the maximum and minimum temperatures by only ~ 30 °C and 40 °C respectively. With a salt surface emissivity of 0.5 -as shown in case 8- the temperatures are only a few degrees lower than for a salt surface emissivity of 1 (case 7). The low impact of the tank on the bottom of the cone could be due to unfavorable view factors and to the low temperature difference between the tank surface and the bottom wall. However, although this difference becomes significant for the upper part, the effect of tank surface on it is still limited especially when compared to other effects such as radiation to the ambient. This suggests that accurately modeling the radiation out of the tank may not be necessary as it doesn't show substantial impact on the FOE wall temperature.

An interesting case shows that passive cooling can be significantly enhanced by applying on the FOE outer wall a paint with high emissivity in the suitable infrared range. Case 10, where this emissivity has been set to 1, shows a significant effect when compared to the base case. A reduction of almost 230 °C and 70 °C for the maximum and minimum temperatures respectively is observed. Even greater reduction is obtained for the case of 0.6 reflectance as shown by comparing cases 1 and 11. The temperature levels obtained after the enhancement in case 10 are low enough to be easily managed with forced-air cooling. This effect will be validated experimentally on the first prototype.

TABLE 1. Cases descriptions and results. * Full description of the variation from base case is in the results section

Case	Description	Variation from base case *	Temperature (°C)	
			Minimum	Maximum
Base	Base case	-	162	529
1	Reflectance effect	Reflectance: $\rho_s = 0.6$	214	711
2	Homogenization effect-Conduction	Conductivity (e.g. glass) $k = 1.4$ W/m/K	106	562
3	Homogenization effect-Conduction	Cone thickness 5 mm	181	520
4	Homogenization effect-Radiation	No internal radiation defined	159	573
5	Homogenization effect-Radiation	Internal radiation: Cone-to-cone only (Tank suppressed, "Perfect" enclosure)	225	527
6	Homogenization effect-Radiation	Internal radiation: cone-to-cone only, inner cone surface emissivity $\varepsilon = 1$	323	466
7	Radiation with tank	Internal radiation: Cone-tank "perfect" enclosure	268	555
8	Radiation with tank	Internal radiation: Cone-tank "perfect" enclosure, salt surface $\varepsilon = 0.5$	262	552
9	Internal Radiation to ambient	Internal radiation: Cone-to-cone open to ambient, tank suppressed	146	490
10	External Radiation	Outer wall emissivity $\varepsilon = 1$	93	302
11	External Radiation	Outer wall emissivity $\varepsilon = 1$, Reflectance: $\rho_s = 0.6$	114	404
12	Internal convection	$h = 5$ W/m^2/K variable T_{air} = [50 °C - 150 °C]	117	468
13	Internal convection	$h = 10$ W/m^2/K variable T_{air} = [50 °C - 150 °C]	94	420
14	Internal convection	Outer wall emissivity $\varepsilon = 1$, $h = 10$ W/m^2/K variable T_{air} = [50 °C - 150 °C]	75	279

Effect of Internal Convection

The following study attempts to develop a sense of sensitivity of the wall temperature to internal convection cooling. The base case, which does not include internal convection, can be assumed to represent a worst case as the internal convection can only have a cooling effect considering the temperature levels reached. This assumes that the internal air temperature T_{air} will not exceed the maximum wall temperature, 507 °C, as the domain is open to air at 50 °C from the top and in contact with the upper tank surfaces at 550 °C. This assumption is no longer obvious for case 10, which represents a high-emissivity outer wall, as temperature of air coming from the tank could be higher than the maximum wall temperature, 302 °C. Yet the following analysis assumes T_{air} at maximum 150 °C in all cases.

Two values of h, 5 and 10 W/m^2/K, have been selected for the sensitivity study in cases 12, 13 and 14 to represent a medium and fair case of convection in the inner domain, based on the order of magnitude of h values calculated for the external convection. As for T_{air}, choosing a constant value on the whole inner domain will not capture the effect of higher cooling at the top which is open to cooler ambient air compared to the bottom in proximity to the hot tank. Hence, values of T_{air} were varied along the 10 slices from 50 °C at the top to 150 °C at the bottom to artificially simulate a variable cooling effect along the FOE height. Comparing cases 12 and 13 to the base case shows a reduction in the maximum temperature of ~ 60 °C and 110 °C respectively. In case of highly emissive outer wall, comparing cases 10 and 14 shows a much more limited effect due to the already low temperatures compared to the base case. This, considering the validity of earlier assumptions, shows a higher effect than the radiation with the tank, but still lower than the external radiation effect using a high emissivity. Therefore, internal convection could be globally considered as having a medium effect and could not be safely neglected.

CONCLUSIONS

A simplified thermal model using ANSYS Mechanical was developed for a cone shaped FOE under 115 kW total incident flux, and different cases have been run to evaluate sensitivity to different parameters. It showed, as expected, that the critical part is located at the bottom of the FOE where the flux density is the highest and resulted in a high temperature difference between top and bottom for the base case.

High conductivity of aluminum proved not sufficient in reducing the temperature difference due to very low thickness to height ratio. Increasing thickness didn't yield significantly lower temperature difference and is therefore not justified. Internal cone-to-cone radiation has a bigger role in reducing the temperature difference than conduction but is still not significant due to the low emissivity of aluminum.

Effect of the radiation exchange with the tank, although representing the maximum possible emission from the tank, proved limited especially compared to effect of radiation to ambient. This suggests that accurately modeling the radiation out of the tank may not be necessary as it doesn't show substantial impact on the FOE wall temperature.

Applying a high emissivity paint on the FOE outer wall was shown to significantly enhance the passive cooling, and consequently reduce the need of active cooling. This effect will be validated experimentally on the first prototype.

A basic sensitivity study of convection in the inner domain showed a medium effect on the maximum temperature, higher than the radiation with the tank but lower than the cooling effect induced by high external emissivity.

The current model inputs will be adapted to conditions of the first prototype testing scheduled for the Fall of 2015 for comparison to experimental results and model adjustment.

ACKNOWLEDGMENTS

The authors would like to acknowledge the work of Vikas Kumar for the ray-tracing optical model of the beam-down system which provided the solar flux input to the current thermal model and for the FOE design.

This work is funded by the Masdar Institute/MIT collaborative flagship project, grant # FR2014-000002.

REFERENCES

1. B. Grange, V. Kumar, A. Gil, P. R. Armstrong, D. S. Codd, A. Slocum and N. Calvet, Energy Procedia **75**, 2163-2168 (2015).
2. M. Mokhtar, S. A. Meyers, P. R. Armstrong and M. Chiesa, J. Sol. Energy Eng. **136** (4), 4-8 (2014).
3. A. H. Slocum, D. S. Codd, J. Buongiorno, C. Forsberg, T. McKrell, J.-C. Nave, C. N. Papanicolas, A. Ghobeity, C. J. Noone, S. Passerini, F. Rojas and A. Mitsos, Sol. Energy **85** (7), 1519-1529 (2011).
4. L. Vant-Hull, Energy Procedia **49**, 257-264 (2014).
5. A. Fernández-García, M. E. Cantos-Soto, M. Röger, C. Wieckert, C. Hutter and L. Martínez-Arcos, Sol. Energy Mater. Sol. Cells **130**, 51-63 (2014).
6. Park Thermal International Corp., "A guide to the safe use of molten salt baths", (ON, Canada, 1996).
7. S. W. Churchill and H. H. S. Chu, Int. J. Heat Mass Transfer **18** (11), 1323-1329 (1975).
8. B. R. Rich, Trans. ASME **75**, 489 (1953).
9. E. M. Sparrow and J. L. Gregg, Trans. ASME **78**, 1823 (1956).